materials

MDPI

Article

Conduction Mechanisms in Au/0.8 nm–GaN/n–GaAs Schottky Contacts in a Wide Temperature Range

Hicham Helal [1,2,*], Zineb Benamara [1], Mouhamed Amine Wederni [3], Sabrine Mourad [4], Kamel Khirouni [4], Guillaume Monier [5], Christine Robert-Goumet [5], Abdelaziz Rabehi [1], Arslane Hatem Kacha [1], Hicham Bakkali [6], Lionel C. Gontard [2] and Manuel Dominguez [2]

1 Laboratoire de Microélectronique Appliquée, Université de Sidi Bel Abbès BP 89, Sidi Bel Abbes 22000, Algeria; benamara20022000@yahoo.fr (Z.B.); rab_ehi@hotmail.fr (A.R.); arslane_k@hotmail.com (A.H.K.)
2 Department of Condensed Matter Physics and IMEYMAT, Institute of Research on Electron Microscopy and Materials, University of Cádiz, Campus Universitario de Puerto Real, E11510 Cádiz, Spain; lionel.cervera@gm.uca.es (L.C.G.); manolo.dominguez@uca.es (M.D.)
3 Unité de recherche Matériaux Avancés et Nanotechnologies (URMAN), Institut Supérieur des Sciences Appliquées et de Technologie de Kasserine, Université de Kairouan, BP 471, Kasserine 1200, Tunisia; wederni.mohamed89@gmail.com
4 Laboratory of Physics of Materials and Nanomaterials Applied to the Environment, Faculty of Sciences of Gabes, University of Gabes, Gabès 6079, Tunisia; sabrine.skmc@gmail.com (S.M.); kamel.khirouni@fsg.rnu.tn (K.K.)
5 Institut Pascal, CNRS, SIGMA Clermont, Université Clermont Auvergne, F-63000 Clermont-Ferrand, France; guillaume.monier@uca.fr (G.M.); christine.robert-goumet@uca.fr (C.R.-G.)
6 Department of Material Science, Metallurgical Engineering and Inorganic Chemistry and IMEYMAT, Institute of Research on Electron Microscopy and Materials, University of Cádiz, Campus Universitario de Puerto Real, E11510 Cádiz, Spain; hicham.bakkali@gm.uca.es
* Correspondence: hichamwartilani@gmail.com

Abstract: Au/0.8 nm–GaN/n–GaAs Schottky diodes were manufactured and electrically characterized over a wide temperature range. As a result, the reverse current I_{inv} increments from 1×10^{-7} A at 80 K to about 1×10^{-5} A at 420 K. The ideality factor n shows low values, decreasing from 2 at 80 K to 1.01 at 420 K. The barrier height $q\phi_b$ grows abnormally from 0.46 eV at 80 K to 0.83 eV at 420 K. The tunnel mechanism TFE effect is the responsible for the $q\phi_b$ behavior. The series resistance R_s is very low, decreasing from 13.80 Ω at 80 K to 4.26 Ω at 420 K. These good results are due to the good quality of the interface treated by the nitridation process. However, the disadvantage of the nitridation treatment is the fact that the GaN thin layer causes an inhomogeneous barrier height.

Keywords: nitridation; GaN/n–GaAs; Schottky diode; I-V-T; conduction mechanisms; barrier height

check for updates

Citation: Helal, H.; Benamara, Z.; Wederni, M.A.; Mourad, S.; Khirouni, K.; Monier, G.; Robert-Goumet, C.; Rabehi, A.; Hatem Kacha, A.; Bakkali, H.; et al. Conduction Mechanisms in Au/0.8 nm–GaN/n–GaAs Schottky Contacts in a Wide Temperature Range. *Materials* **2021**, *14*, 5909. https://doi.org/10.3390/ma14205909

Academic Editor: Bertrand Lenoir

Received: 7 September 2021
Accepted: 1 October 2021
Published: 9 October 2021

Publisher's Note: MDPI stays neutral with regard to jurisdictional claims in published maps and institutional affiliations.

Copyright: © 2021 by the authors. Licensee MDPI, Basel, Switzerland. This article is an open access article distributed under the terms and conditions of the Creative Commons Attribution (CC BY) license (https://creativecommons.org/licenses/by/4.0/).

1. Introduction

Metal-semiconductor (MS) contacts are very important in microelectronics [1–4]. They are used in optoelectronic devices, bipolar integrated circuits, high-temperature, and high-frequency applications [5,6]. The thermionic emission (TE) theory is the principal theory used to determine the parameters of the Schottky contact.

However, the experimental current-voltage (I-V) characteristics present some anomalies at low temperatures, and both the Schottky barrier height and ideality factor are temperature-dependent [5,7–10].

This deviation of the thermionic emission theory is corrected by introducing other mechanisms, operating at the Schottky barrier such as the thermionic field emission TFE and the emission field FE currents [5,11].

The origin of these currents is explained by considering several phenomena. First, the Schottky barrier is typically not homogeneous in space [7,12–15], as measured using ballistic electron emission microscopy [16,17]. The most widely accepted approach for

interpreting experimental data considers that the spatial barrier inhomogeneity can be modeled with a Gaussian distribution function [12,18–24].

Secondly, the existence of interface states [7,25] act as recombination centers and generate local electric fields, causing random metallic paths, reducing carrier lifetime, and inducing a large leakage current [26–29]. These interface states come from surface dislocations and surface contaminations incorporated during the elaboration process [27,30,31]. In addition, the Schottky metallization step can cause interfacial modifications [31–34].

Therefore, the interface quality has an essential impact on device behavior and performance. In this context, surface passivation is the best method of controlling the defective states [27,30,31,35–39]., Many studies on the nitridation of the GaAs surface have been carried out [27,30,37,38,40–43] to improve the behavior and the electrical properties of the Schottky contacts (e.g., the ideality factor, barrier height, saturation current, series resistance and reverse current. Moreover, the nitride layers have good stability against the formation of amorphous surface oxides, high electronegativity, and thermal stability [27,44].

In this work, we measure the electrical characteristics of Au/0.8 nm–GaN/n–GaAs Schottky contacts fabricated by using a glow-discharge plasma source (GDS) for nitridation. Moreover, we analyze the current transport mechanisms, and several electrical parameters are characterized in a wide range of temperatures (80–420 K).

2. The Experiment

The Schottky contacts were elaborated using commercially available Si-doped n-GaAs (100) substrates, of a thickness of 400 µm and an electron concentration $N_d = 4.9 \times 10^{15}$ cm^{-3}. The samples were cleaned chemically using H_2SO_4, deionized water, cold and hot methanol sequentially and dried with N_2. Then, the surfaces were bombarded with Ar+ ions of about 1 keV (a sample current equal to 5 µA cm^{-2} during 1 h) in UHV conditions [30,40]. After surface cleaning, the substrates were heated at 500 °C and nitrided using a glow discharge nitrogen plasma source, running at 5 W for 30 min in a UHV chamber (Institut Pascal, Clermont-Ferrand, France). This nitridation process led to the growth of a 0.8 nm-thick layer of undoped GaN. Following the nitridation step, the samples were annealed at 620 °C for 1 h to crystallize the GaN layer [39,45,46].

A XPS system characterized by a dual anode Al–Mg X-ray source (Institut Pascal, Clermont-Ferrand, France) and hemispherical electron energy analyzer (Institut Pascal, Clermont-Ferrand, France) were used for the in situ measurement of the chemical composition and crystal structure. The GaN thickness was calculated by comparing the experimental spectra data to the theoretical XPS peak intensities and positions [38]. The Au dots were deposited with area of 4.41×10^{-3} cm^2 and thickened to 100 nm. A Bruker Dimension Icon atomic force microscope (AFM, Bruker, Cádiz, Spain) equipped with ScanAsyst and Nanoscope software 9.7 (ScanAsyst, Cádiz, Spain) was used to investigate the film surface roughness. Using the PeakForce tapping mode, AFM topography measurements were taken in the air. To accomplish this, a silicon tip on a nitride cantilever (ScanAsyst Air model, Cádiz, Spain), with a 0.4 N m^{-1} spring constant and a nominal tip radius of 2 nm were used to examine regions of 1×1 µm^2 with a resolution of 256×256 pixels. The current–voltage measurements were investigated under different temperatures (80–420 K), by a current source Keithely 220 (Laboratory of Physics of Materials and Nanomaterials Applied to the Environment, Gabès, Tunisia).

3. The Results

Figure 1 presents the PeakForce tapping AFM topography images for (a) the GaN surface and (b) an Au electrode within a 1×1 µm^2 scan area represented at the same height scale. The Au texture was formed by interconnected grain channels, while that of GaN was almost flat. The root mean square (RMS) surface roughness values indicated a difference of almost one order of magnitude between Au and GaN smoothness, i.e., 0.3 nm for GaN and 4.6 nm for Au. The value of the RMS surface roughness for GaN was calculated by neglecting the areas occupied by the contamination features that clearly stand

out in the Figure 1a. This value of roughness (0.3 nm) is less than half the nominal GaN layer thickness (0.8 nm).

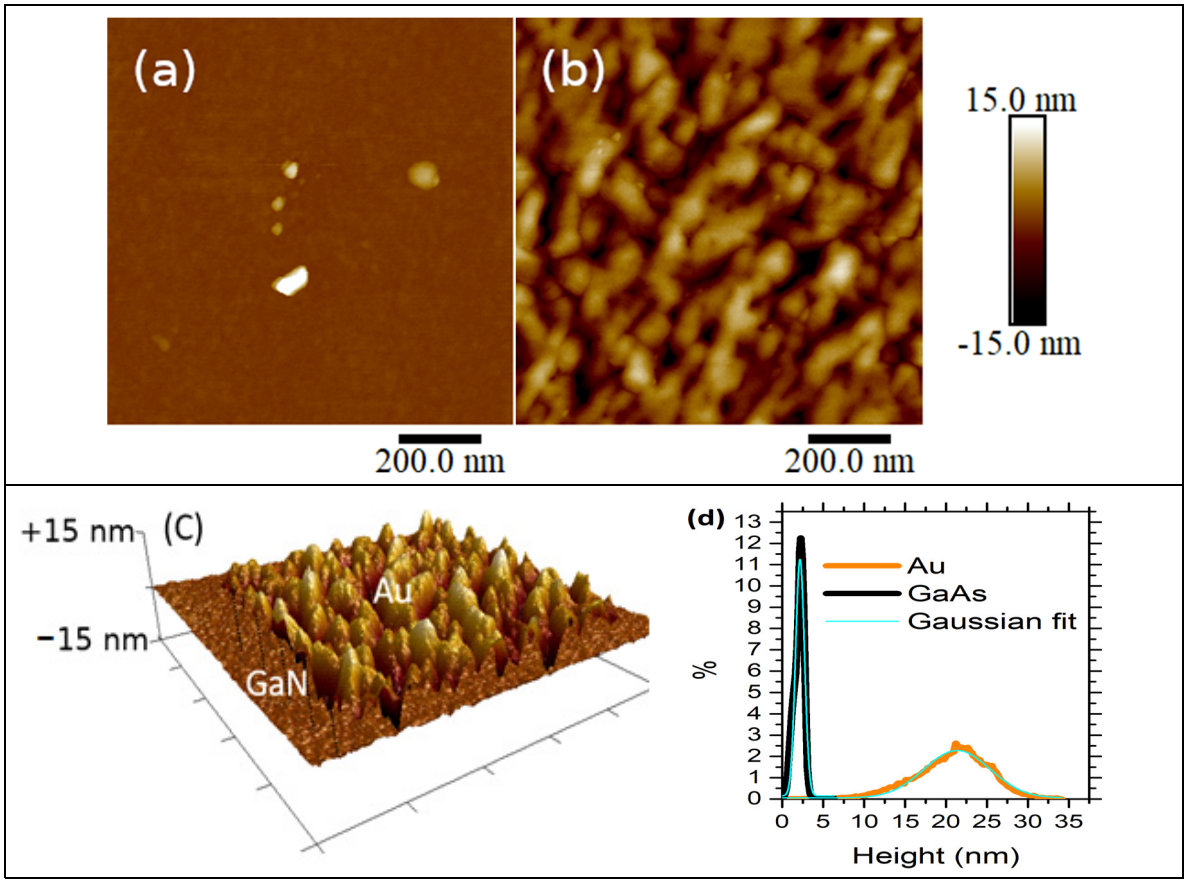

Figure 1. PeakForce tapping AFM topography for (**a**) GaN, and (**b**) Au surfaces. (**c**) Rendered illuminated 3D AFM image of GaN/Au frontier. (**d**) Height distribution functions obtained from the topography images.

The roughness difference is better shown in Figure 1c where the frontier between the Au electrode and the GaN surface is shown as a rendered illuminated 3D AFM image, and the different topographies of Au and GaN are clearly shown. To bring out this difference in roughness more clearly, the height distribution histograms shown in Figure 1d were obtained from the topography images. GaN exhibits a narrow peak, showing that in comparison to Au, which has a larger peak, the surface layer is more homogeneous. To clarify the difference between the peaks, they have been fitted to a single Gaussian distribution with a peak centered at 2.15, and 21.3 nm, and a full width at half maximum (FWHM) of 1.3 and 9.5 nm for GaN and Au, respectively.

Surface roughness induces a non-uniformity of thickness, a distribution of interfacial charges, and a local variation of the Fermi level. These phenomena yield to the inhomogeneity of the Schottky barrier height and affect the transport mechanism [47].

Figure 2 depicts the I-V characteristics of the Au/0.8 nm–GaN/n–GaAs structure, at temperatures ranging from 80 to 420 K.

The values of the reverse current I_{Rev} at −1 V and the threshold voltage V_{Th} were extracted and illustrated in Figure 3. With increasing temperature, I_{Rev} increased exponentially from 1×10^{-7} A at 80 K to 1×10^{-5} A at 420 K, and V_{Th} decreased from 0.65 V at 80 K to 0.2 V at 420 K.

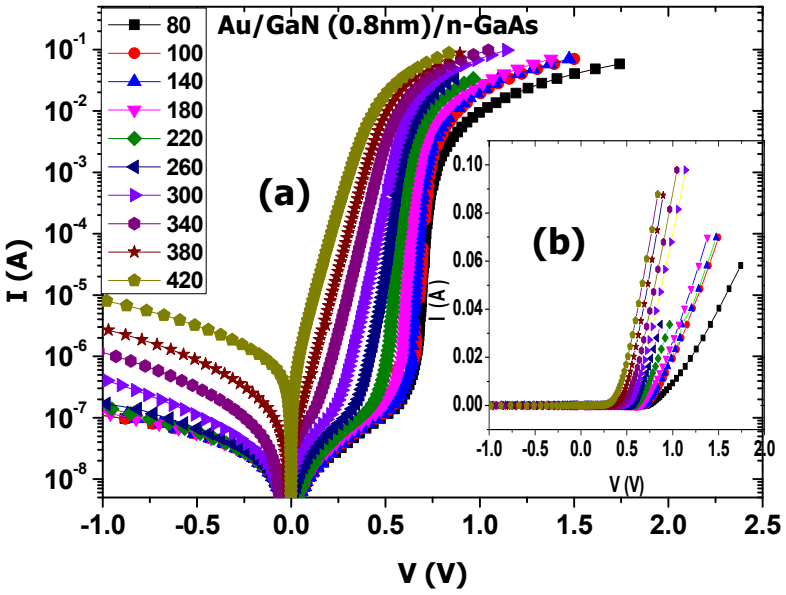

Figure 2. I−V measurements of Au/0.8 nm–GaN/n–GaAs structure, (**a**) semi-logarithmic scale and (**b**) linear scale.

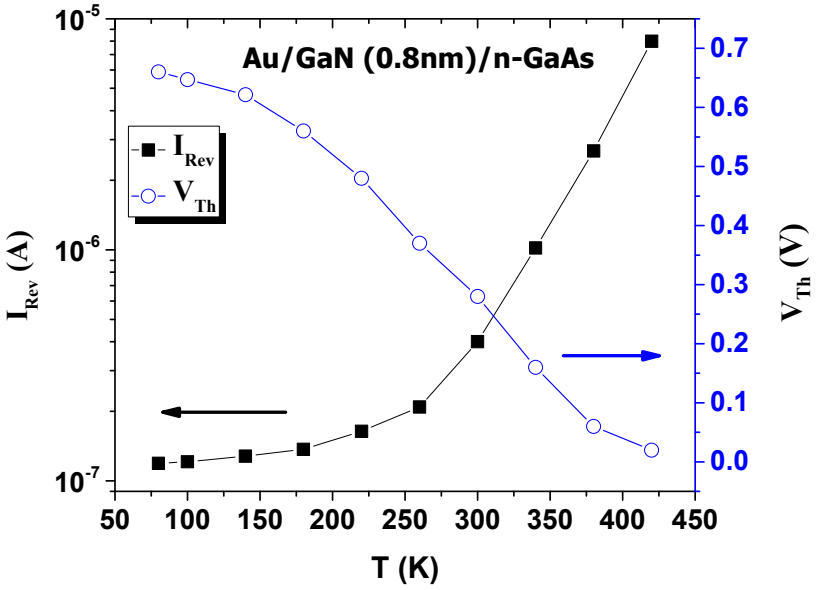

Figure 3. Variation of reverse leakage current and threshold voltage versus temperature.

The expression of the current for non-ideal Schottky diodes is [48]:

$$I = I_s\left(exp\left(\frac{q(V - IR_s)}{nkT}\right) - 1\right) \quad (1)$$

and

$$I_s = AA^*T^2\left(-\frac{q\phi_b}{kT}\right) \quad (2)$$

where, I_s is the saturation current; R_s is the series resistance; $q\phi_b$ is the barrier height; n is the ideality factor; k is the Boltzmann constant; A is the effective diode area, and A^* is the effective Richardson constant equal to 8.16 $Acm^{-2}K^2$ for GaAs.

At the low bias voltage V, the current I is low, therefore the term IR_s is low compared to V, and (Equation (1)) becomes

$$I = I_s exp\left(\frac{qV}{nkT}\right) \tag{3}$$

and

$$ln(I) = \frac{q}{nkT}V + ln(I_s) \tag{4}$$

The n and I_s values are calculated from the slope and y-intercept of $ln(I)$-V, respectively. The ϕ_b value is determined as follows:

$$\phi_b = \frac{kT}{q} ln\left(\frac{AA^*T^2}{I_s}\right) \tag{5}$$

The R_s values are extracted using the Cheung and Cheung method [48] which is based on

$$G(I) = \frac{\partial V}{\partial(lnI)} = R_s I + \frac{nkT}{q} \tag{6}$$

The extracted values of n and $q\phi_b$ are plotted in Figure 4.

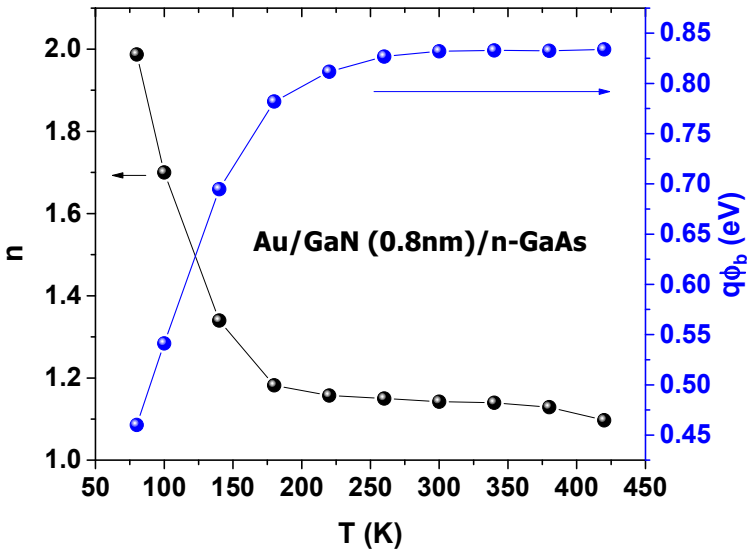

Figure 4. The n and ϕ_b extracted at each temperature.

As can be seen from Figure 4, with the rising temperature, n dropped from 2 for 80 K to 1.1 for 420 K. The decrease was very slow from 250 K to 450 K, which is in accordance with the literature [5–7,11,26]. The low values of n may have been due to the effect of the nitridation process, which improves the quality of the interface. As the temperature rose, $q\phi_b$ rose abnormally from 0.46 eV for 80 K to 0.83 eV for 420 K. These results were similar to several studies [7,12,20,49–51]. For Schottky contacts, the $q\phi_b$ value should decrease as the temperature rises, due to the bandgap's temperature variation [1,2,7,48,50,52–54]. The $q\phi_b$ behavior may be explained by tunnel effect mechanisms, such as thermionic field emission (TFE) [5,11].

The tunneling current can be expressed following [1,12,55,56] as

$$I = I_{tun}\left[exp\left(\frac{q(V - IR_s)}{E_0}\right) - 1\right] \tag{7}$$

$$\frac{E_0}{kT} = \frac{E_{00}}{kT} cot\, h\left(\frac{E_{00}}{kT}\right) \tag{8}$$

$$E_{00} = \frac{h}{4\pi}\left(\frac{N_D}{m_e^* \varepsilon_s}\right)^{\frac{1}{2}} \quad (9)$$

where E_{00} is the characteristic tunneling energy; h is the Planck constant; m_e^* is the effective mass of electron; and ε_s is the dielectric constant of GaAs. Figure 5 shows the variation of $(E_0 = nkT/q)$ versus kT/q.

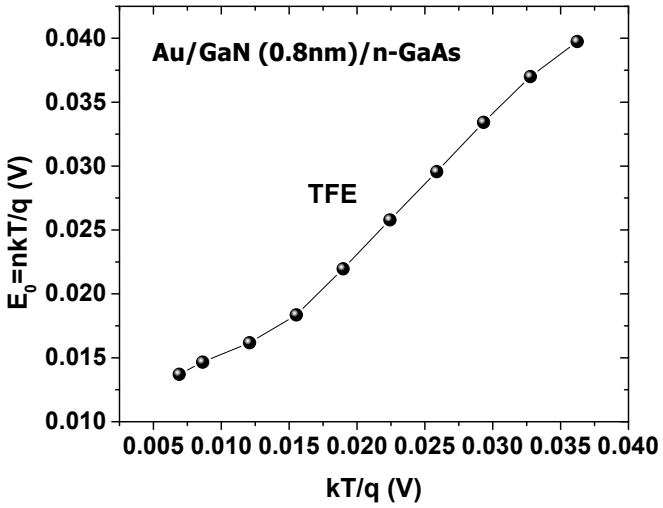

Figure 5. Variation of E_0 (nkT/q) versus kT/q.

From Figure 5, E_0 is about kT/q, which confirms that the TFE mechanism is dominant [26], not the theoretical mechanism TE of the Schottky contacts. This explains the abnormal behavior of the barrier height and the deviation of the ideality factor from unity. This may have been due to the interface states, which behaved as recombination–generation centers that affected the conduction mechanism [57].

To further study the abnormal behavior of the barrier height, the Richardson characteristic $ln(I_s/T^2)$ versus q/kT is presented in Figure 6 using the equation

$$ln\left(\frac{I_s}{T^2}\right) = ln(AA^*) - q\frac{\phi_{b_n}}{kT} \quad (10)$$

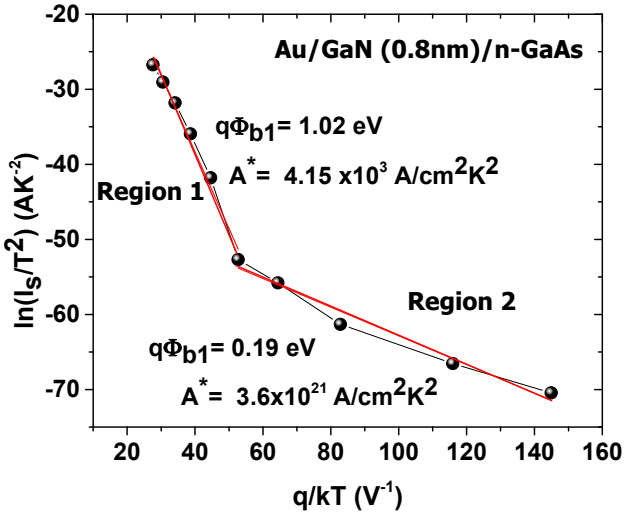

Figure 6. Variation of Richardson characteristic $ln(I_s/T^2)$ versus q/kT. Red lines are linear fits of experimental data according to the root mean square method.

Figure 6 gives two linear regions which are due to the inhomogeneity of the barrier height [12]. $q\phi_b$ and A^* values are 1.02 eV and 4.15 × 10^3 $Acm^{-2}K^{-2}$ respectively in region 1 and equal to 0.19 eV and 3.6 × 10^{21} $Acm^{-2}K^{-2}$ respectively in region 2. These values of A^* are significantly far from the theoretical value 8.16 $Acm^{-2}K^{-2}$ for n-GaAs [52].

Figure 7 presents the variation of ϕ_b versus n.

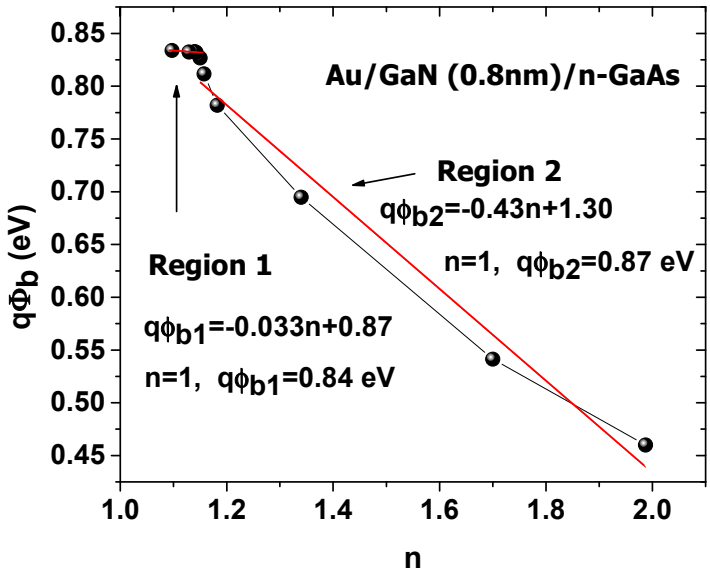

Figure 7. ϕ_b versus n.

The structure has two linear characteristics due to barrier height inhomogeneity [58,59]. By extrapolation, the estimated values of $q\phi_b$ for n = 1 are 0.87 eV for region 1, and 0.84 eV for region 2. These values are closer than those extracted from the Richardson characteristics.

The authors of this work [5] previously performed simulations of Au/n–GaAs Schottky at temperatures ranging from 80 to 400 K, with and without a thin GaN (1 nm) interfacial layer. They found that Au/n–GaAs shows a homogeneous barrier height while Au/1 nm–GaN/n–GaAs structure shows an inhomogeneous one. Therefore, the experimental results shown here—-the inhomogeneity of the barrier height shown in the Richardson characteristics and in the plot of $q\phi_b$ versus n—-are most likely because of the 0.8 nm GaN layer. Figure 8 illustrates *G(I)* plots of the Cheung and Cheung method at temperatures 80–420 K.

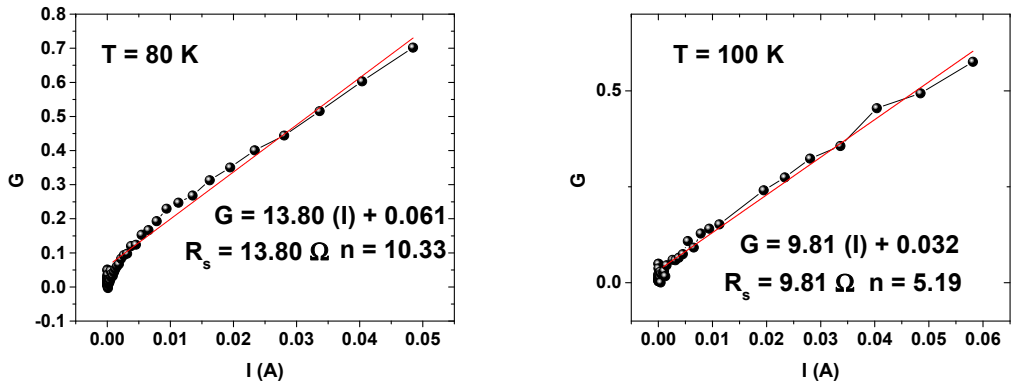

Figure 8. *Cont.*

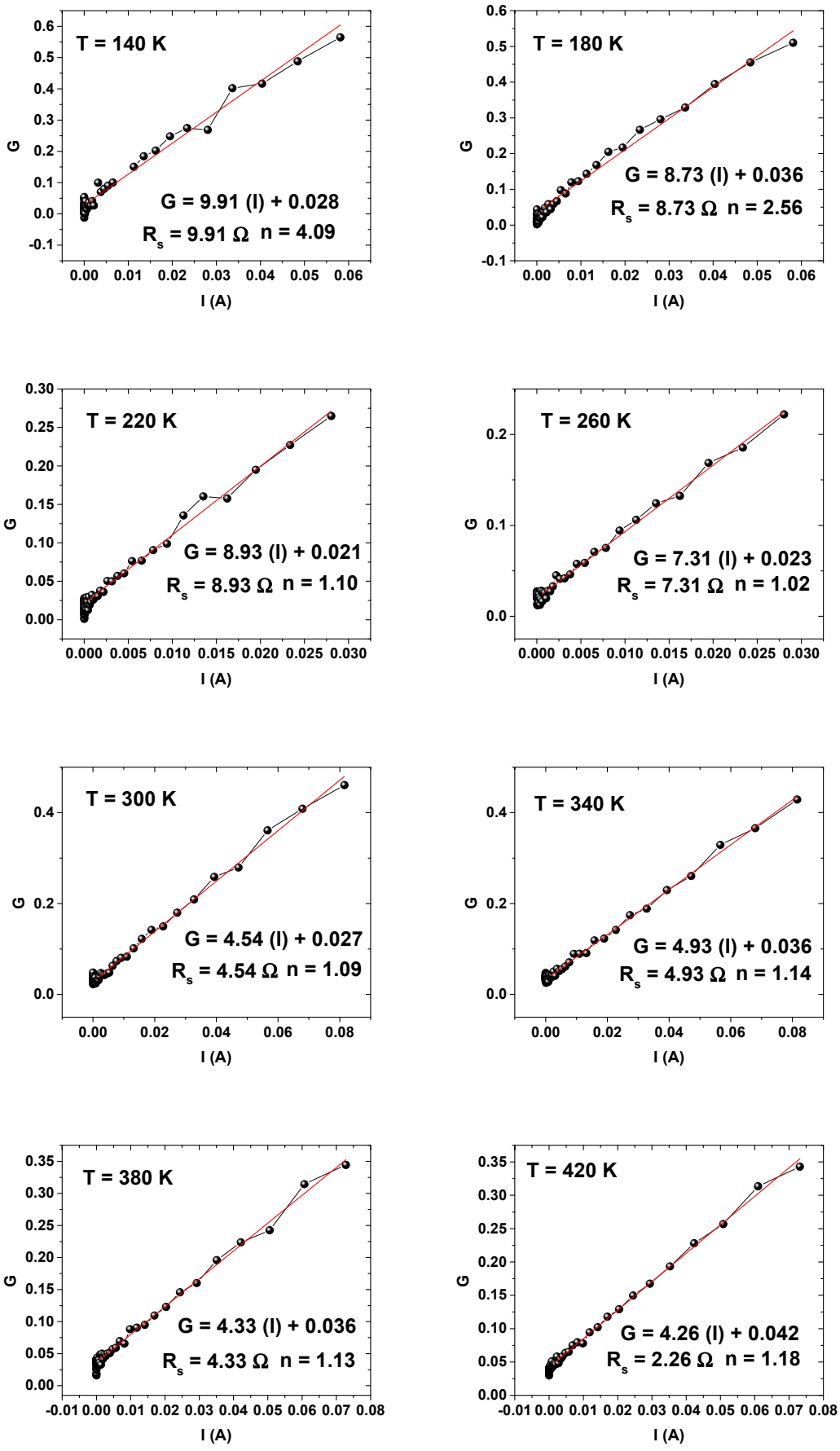

Figure 8. *dV/d(lnI)* plots at different temperatures.

R_s and n were extracted by the Cheung and Cheung method for each temperature and presented in Figures 9 and 10, respectively.

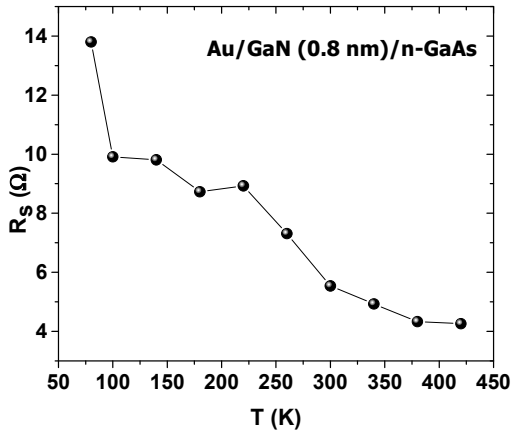

Figure 9. R_s (Cheung and Cheung method) versus temperature.

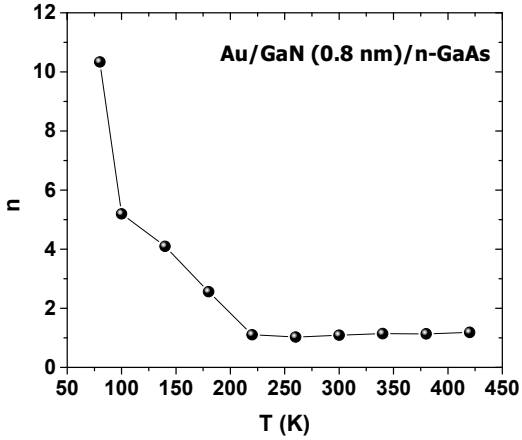

Figure 10. n (Cheung and Cheung method) versus temperature.

As can be seen, the structure gives the low resistance series R_s, which decreased from 13.80 Ω at 80 K to 4.26 Ω at 420 K, showing the good quality of the interface improved by nitridation and annealing [28].

The n values were very high at low temperatures compared to those extracted from the first method. This discrepancy occurred because the n values obtained by the first method were extracted from the low bias voltage range, where the series resistance is very low. On the other hand, the n values extracted using the Cheung and Cheung method were extracted from all bias voltage ranges, where the series resistance in high bias voltages affects the calculation of the ideality factor.

Finally, the growth of a 0.8 nm of GaN layer on n-GaAs surfaces with an annealing process led to improved electrical parameters of the Schottky contacts, such as the series resistance and the ideality factor. However, it can cause the inhomogeneity of the barrier height at the structure.

4. Conclusions

Au/0.8 nm–GaN/n–GaAs structures were fabricated using a glow discharge plasma source (GDS), and their current–voltage characteristics were investigated for different temperatures. The samples showed good electrical parameters where n decreased from 2 for 80 K to 1.01 for 420 K. The barrier height $q\phi_b$ grew abnormally from 0.46 eV at 80 K to 0.83 eV at 420 K, due to the tunnel mechanism TFE effect. In addition, the samples showed

low R_s which dropped from 13.80 Ω at 80 K to 4.26 Ω at 420 K. Finally, the results strongly suggested that the GaN thin layer caused an inhomogeneous barrier height, which was also in agreement with our previous simulations [5].

Author Contributions: Conceptualization, H.H.; methodology, H.H.; software, H.B.; validation, H.H.; formal analysis, H.H.; investigation, K.K., M.D., L.C.G. and C.R.-G.; resources, M.D.; data curation, M.A.W., S.M., A.H.K., A.R.; writing—original draft preparation, H.H.; writing—review and editing, H.H., M.D. and G.M.; visualization, H.B.; supervision, Z.B. and M.D.; project administration, Z.B.; funding acquisition, M.D. and C.R.-G. All authors have read and agreed to the published version of the manuscript.

Funding: H. Bakkali, L.C. Gontard and M. Dominguez acknowledge funding from the University of Cadiz and from the regional government Junta de Andalucia (reference PAI FQM335). M. Dominguez acknowledges financial support from the Spanish Ministry of Science and Innovation under project reference EQC2018-004704-P FEDER 2014-2020.

Institutional Review Board Statement: Not applicable.

Informed Consent Statement: Not applicable.

Data Availability Statement: The data presented in this study are available on request from the corresponding author.

Acknowledgments: The authors wish to thank Soumaya Ayachi, Oumayma Amorri and the entire team of the Laboratory of Physics of Materials and Nanomaterials Applied to the Environment, Gabes University, Tunisia.

Conflicts of Interest: The authors declare no conflict of interest.

References

1. Rhoderick, E.; Williams, R. *Metal–Semiconductor Contacts*; Clarendon Press: Oxford, UK, 1988.
2. Sze, S.M.; Ng, K.K. *Physics of Semiconductor Devices*; John Wiley & Sons: Hobocken, NJ, USA, 2006.
3. Demircioglu, Ö.; Karataş, Ş.; Yıldırım, N.; Bakkaloglu, Ö.; Türüt, A. Temperature dependent current–voltage and capacitance–voltage characteristics of chromium Schottky contacts formed by electrodeposition technique on n-type Si. *J. Alloy. Compd.* **2011**, *509*, 6433–6439. [CrossRef]
4. Korucu, D.; Turut, A.; Altındal, Ş. The origin of negative capacitance in Au/n-GaAs Schottky barrier diodes (SBDs) prepared by photolithography technique in the wide frequency range. *Curr. Appl. Phys.* **2013**, *13*, 1101–1108. [CrossRef]
5. Helal, H.; Benamara, Z.; Arbia, M.B.; Khettou, A.; Rabehi, A.; Kacha, A.H.; Amrani, M. A study of current-voltage and capacitance-voltage characteristics of Au/n-GaAs and Au/GaN/n-GaAs Schottky diodes in wide temperature range. *Int. J. Numer. Model. Electron. Netw. Devices Fields* **2020**, *33*, e2714. [CrossRef]
6. Zeyrek, S.; Bülbül, M.; Altındal, Ş.; Baykul, M.; Yüzer, H. The double gaussian distribution of inhomogeneous barrier heights in Al/GaN/p-GaAs (MIS) schottky diodes in wide temperature range. *Braz. J. Phys.* **2008**, *38*, 591–597.
7. Hardikar, S.; Hudait, M.; Modak, P.; Krupanidhi, S.; Padha, N. Anomalous current transport in Au/low-doped n-GaAs Schottky barrier diodes at low temperatures. *Appl. Phys.* **1999**, *68*, 49–55. [CrossRef]
8. Kumar, A.; Arafin, S.; Amann, M.C.; Singh, R. Temperature dependence of electrical characteristics of Pt/GaN Schottky diode fabricated by UHV e-beam evaporation. *Nanoscale Res. Lett.* **2013**, *8*, 481. [CrossRef]
9. Osvald, J.; Horvath, Z.J. Theoretical study of the temperature dependence of electrical characteristics of Schottky diodes with an inverse near-surface layer. *Appl. Surf. Sci.* **2004**, *234*, 349–354. [CrossRef]
10. Tunhuma, S.M.; Auret, F.D.; Legodi, M.J.; Diale, M. The effect of high temperatures on the electrical characteristics of Au/n-GaAs Schottky diodes. *Phys. B Condens. Matter* **2016**, *480*, 201–205. [CrossRef]
11. Özavcı, E.; Demirezen, S.; Aydemir, U.; Altındal, Ş. A detailed study on current–voltage characteristics of Au/n-GaAs in wide temperature range. *Sens. Actuators A Phys.* **2013**, *194*, 259–268. [CrossRef]
12. Werner, J.H.; Güttler, H.H. Barrier inhomogeneities at Schottky contacts. *J. Appl. Phys.* **1991**, *69*, 1522–1533. [CrossRef]
13. Sullivan, J.; Tung, R.; Pinto, M.; Graham, W. Electron transport of inhomogeneous Schottky barriers: A numerical study. *J. Appl. Phys.* **1991**, *70*, 7403–7424. [CrossRef]
14. Tung, R. Electron transport at metal-semiconductor interfaces: General theory. *Phys. Rev.* **1992**, *45*, 13509. [CrossRef]
15. Schmitsdorf, R.; Kampen, T.; Mönch, W. Explanation of the linear correlation between barrier heights and ideality factors of real metal-semiconductor contacts by laterally nonuniform Schottky barriers. *J. Vac. Sci. Technol. B Microelectron. Nanometer Struct. Process. Meas. Phenom.* **1997**, *15*, 1221–1226. [CrossRef]
16. Palm, H.; Arbes, M.; Schulz, M. Fluctuations of the Au-Si (100) Schottky barrier height. *Phys. Rev. Lett.* **1993**, *71*, 2224. [CrossRef]

17. Vanalme, G.; Goubert, L.; van Meirhaeghe, R.; Cardon, F.; van Daele, P. A ballistic electron emission microscopy study of barrier height inhomogeneities introduced in Au/III-V semiconductor Schottky barrier contacts by chemical pretreatments. *Semicond. Sci. Technol.* **1999**, *14*, 871. [CrossRef]
18. Chin, V.W.; Green, M.; Storey, J.W. Evidence for multiple barrier heights in P-type PtSi Schottky-barrier diodes from IVT and photoresponse measurements. *Solid-State Electron.* **1990**, *33*, 299–308. [CrossRef]
19. Singh, A.; Reinhardt, K.; Anderson, W. Temperature dependence of the electrical characteristics of Yb/p-InP tunnel metal-insulator-semiconductor junctions. *J. Appl. Phys.* **1990**, *68*, 3475–3483. [CrossRef]
20. Chand, S.; Kumar, J. Current transport in Pd 2 Si/n-Si (100) Schottky barrier diodes at low temperatures. *Appl. Phys.* **1996**, *63*, 171–178. [CrossRef]
21. McCafferty, P.; Sellai, A.; Dawson, P.; Elabd, H. Barrier characteristics of PtSip-Si Schottky diodes as determined from IVT measurements. *Solid-State Electron.* **1996**, *39*, 583–592. [CrossRef]
22. Zhu, S.; van Meirhaeghe, R.; Detavernier, C.; Ru, G.-P.; Li, B.-Z.; Cardon, F. A BEEM study of the temperature dependence of the barrier height distribution in PtSi/n-Si Schottky diodes. *Solid state Commun.* **1999**, *112*, 611–615. [CrossRef]
23. Zhu, S.; van Meirhaeghe, R.; Detavernier, C.; Cardon, F.; Ru, G.-P.; Qu, X.-P.; Li, B.-Z. Barrier height inhomogeneities of epitaxial CoSi2 Schottky contacts on n-Si (100) and (111). *Solid-State Electron.* **2000**, *44*, 663–671. [CrossRef]
24. Korucu, D.; Turut, A.; Efeoglu, H. Temperature dependent I–V characteristics of an Au/n-GaAs Schottky diode analyzed using Tung's model. *Phys. B Condens. Matter* **2013**, *414*, 35–41. [CrossRef]
25. Crowell, C. The physical significance of the T0 anomalies in Schottky barriers. *Solid-State Electron.* **1977**, *20*, 171–175. [CrossRef]
26. Hudait, M.; Venkateswarlu, P.; Krupanidhi, S. Electrical transport characteristics of Au/n-GaAs Schottky diodes on n-Ge at low temperatures. *Solid-State Electron.* **2001**, *45*, 133–141. [CrossRef]
27. Helal, H.; Benamara, Z.; Kacha, A.H.; Amrani, M.; Rabehi, A.; Akkal, B.; Monier, G.; Robert-Goumet, C. Comparative study of ionic bombardment and heat treatment on the electrical behavior of Au/GaN/n-GaAs Schottky diodes. *Superlattices Microstruct.* **2019**, *135*, 106276. [CrossRef]
28. Uslu, H.; Bengi, A.; Çetin, S.; Aydemir, U.; Altındal, Ş.; Aghaliyeva, S.; Özçelik, S. Temperature and voltage dependent current-transport mechanisms in GaAs/AlGaAs single-quantum-well lasers. *J. Alloy. Compd.* **2010**, *507*, 190–195. [CrossRef]
29. Dawidowski, W.; Ściana, B.; Bielak, K.; Mikolášek, M.; Drobný, J.; Serafińczuk, J.; Lombardero, I.; Radziewicz, D.; Kijaszek, W.; Kósa, A. Analysis of Current Transport Mechanism in AP-MOVPE Grown GaAsN pin Solar Cell. *Energies* **2021**, *14*, 4651. [CrossRef]
30. Rabehi, A.; Amrani, M.; Benamara, Z.; Akkal, B.; Hatem-Kacha, A.; Robert-Goumet, C.; Monier, G.; Gruzza, B. Study of the characteristics current-voltage and capacitance-voltage in nitride GaAs Schottky diode. *Eur. Phys. J. Appl. Phys.* **2015**, *72*, 10102. [CrossRef]
31. Güllü, Ö.; Biber, M.; Duman, S.; Türüt, A. Electrical characteristics of the hydrogen pre-annealed Au/n-GaAs Schottky barrier diodes as a function of temperature. *Appl. Surf. Sci.* **2007**, *253*, 7246–7253. [CrossRef]
32. Ayyildiz, E.; Cetin, H.; Horvath, Z.J. Temperature dependent electrical characteristics of Sn/p-Si Schottky diodes. *Appl. Surf. Sci.* **2005**, *252*, 1153–1158. [CrossRef]
33. Horvath, Z.J.; Rakovics, V.; Szentpali, B.; Püspöki, S.; Žd'ánský, K. InP Schottky junctions for zero bias detector diodes. *Vacuum* **2003**, *71*, 113–116. [CrossRef]
34. Altındal, Ş.; Karadeniz, S.; Tuğluoğlu, N.; Tataroğlu, A. The role of interface states and series resistance on the I–V and C–V characteristics in Al/SnO2/p-Si Schottky diodes. *Solid-State Electron.* **2003**, *47*, 1847–1854. [CrossRef]
35. Matolın, V.; Fabık, S.; Glosık, J.; Bideux, L.; Ould-Metidji, Y.; Gruzza, B. Experimental system for GaN thin films growth and in situ characterisation by electron spectroscopic methods. *Vacuum* **2004**, *76*, 471–476. [CrossRef]
36. Ould-Metidji, Y.; Bideux, L.; Baca, D.; Gruzza, B.; Matolin, V. Nitridation of GaAs (1 0 0) substrates and Ga/GaAs systems studied by XPS spectroscopy. *Appl. Surf. Sci.* **2003**, *212*, 614–618. [CrossRef]
37. Benamara, Z.; Mecirdi, N.; Bouiadjra, B.B.; Bideux, L.; Gruzza, B.; Robert, C.; Miczek, M.; Adamowicz, B. XPS, electric and photoluminescence-based analysis of the GaAs (1 0 0) nitridation. *Appl. Surf. Sci.* **2006**, *252*, 7890–7894. [CrossRef]
38. Kacha, A.; Akkal, B.; Benamara, Z.; Amrani, M.; Rabhi, A.; Monier, G.; Robert-Goumet, C.; Bideux, L.; Gruzza, B. Effects of the GaN layers and the annealing on the electrical properties in the Schottky diodes based on nitrated GaAs. *Superlattices Microstruct.* **2015**, *83*, 827–833. [CrossRef]
39. Mehdi, H.; Monier, G.; Hoggan, P.; Bideux, L.; Robert-Goumet, C.; Dubrovskii, V. Combined angle-resolved X-ray photoelectron spectroscopy, density functional theory and kinetic study of nitridation of gallium arsenide. *Appl. Surf. Sci.* **2018**, *427*, 662–669. [CrossRef]
40. Rabehi, A.; Amrani, M.; Benamara, Z.; Akkal, B.; Kacha, A. Electrical and photoelectrical characteristics of Au/GaN/GaAs Schottky diode. *Optik* **2016**, *127*, 6412–6418. [CrossRef]
41. Ambrico, M.; Losurdo, M.; Capezzuto, P.; Bruno, G.; Ligonzo, T.; Haick, H. Probing electrical properties of molecule-controlled or plasma-nitrided GaAs surfaces: Two different tools for modifying the electrical characteristics of metal/GaAs diodes. *Appl. Surf. Sci.* **2006**, *252*, 7636–7641. [CrossRef]
42. Bideux, L.; Monier, G.; Matolin, V.; Robert-Goumet, C.; Gruzza, B. XPS study of the formation of ultrathin GaN film on GaAs (1 0 0). *Appl. Surf. Sci.* **2008**, *254*, 4150–4153. [CrossRef]

43. Kacha, A.; Akkal, B.; Benamara, Z.; Robert-Goumet, C.; Monier, G.; Gruzza, B. Study of the surface state density and potential in MIS diode Schottky using the surface photovoltage method. *Mol. Cryst. Liq. Cryst.* **2016**, *627*, 66–73. [CrossRef]
44. Berkovits, V.; L'vova, T.; Ulin, V. Chemical nitridation of GaAs (100) by hydrazine-sulfide water solutions. *Vacuum* **2000**, *57*, 201–207. [CrossRef]
45. Monier, G.; Bideux, L.; Robert-Goumet, C.; Gruzza, B.; Petit, M.; Lábár, J.; Menyhárd, M. Passivation of GaAs (001) surface by the growth of high quality c-GaN ultra-thin film using low power glow discharge nitrogen plasma source. *Surf. Sci.* **2012**, *606*, 1093–1099. [CrossRef]
46. Mehdi, H.; Réveret, F.; Bougerol, C.; Robert-Goumet, C.; Hoggan, P.; Bideux, L.; Gruzza, B.; Leymarie, J.; Monier, G. Study of GaN layer crystallization on GaAs (100) using electron cyclotron resonance or glow discharge N2 plasma sources for the nitriding process. *Appl. Surf. Sci.* **2019**, *495*, 143586. [CrossRef]
47. Ozdemir, M.; Sevgili, O.; Orak, I.; Turut, A. Determining the potential barrier presented by the interfacial layer from the temperature induced IV characteristics in Al/p-Si Structure with native oxide layer. *Mater. Sci. Semicond. Process.* **2021**, *125*, 105629. [CrossRef]
48. Cheung, S.; Cheung, N. Extraction of Schottky diode parameters from forward current-voltage characteristics. *Appl. Phys. Lett.* **1986**, *49*, 85–87. [CrossRef]
49. Horváth, Z.J. A New Approach to Temperature Dependent Ideality Factors in Schottky Contacts. *MRS Online Proc. Libr. Arch.* **1992**, *260*, 359–366. [CrossRef]
50. Hackam, R.; Harrop, P. Electrical properties of nickel-low-doped n-type gallium arsenide Schottky-barrier diodes. *IEEE Trans. Electron. Devices* **1972**, *19*, 1231–1238. [CrossRef]
51. Bhuiyan, A.; Martinez, A.; Esteve, D. A new Richardson plot for non-ideal schottky diodes. *Thin Solid Film.* **1988**, *161*, 93–100. [CrossRef]
52. Bengi, A.; Altındal, S.; Özçelik, S.; Mammadov, T. Gaussian distribution of inhomogeneous barrier height in Al0. 24Ga0. 76As/GaAs structures. *Phys. B Condens. Matter* **2007**, *396*, 22–28. [CrossRef]
53. Werner, J.H. Schottky barrier and pn-junctionI/V plots—Small signal evaluation. *Appl. Phys.* **1988**, *47*, 291–300. [CrossRef]
54. Panish, M.; Casey, H.C., Jr. Temperature dependence of the energy gap in GaAs and GaP. *J. Appl. Phys.* **1969**, *40*, 163–167. [CrossRef]
55. Padovani, F.; Sumner, G. Experimental Study of Gold-Gallium Arsenide Schottky Barriers. *J. Appl. Phys.* **1965**, *36*, 3744–3747. [CrossRef]
56. Padovani, F. Graphical determination of the barrier height and excess temperature of a Schottky barrier. *J. Appl. Phys.* **1966**, *37*, 921–922. [CrossRef]
57. Ebeoğlu, M.A. Current–voltage characteristics of Au/GaN/GaAs structure. *Phys. B Condens. Matter* **2008**, *403*, 61–66. [CrossRef]
58. Schmitsdorf, R.; Kampen, T.; Mönch, W. Correlation between barrier height and interface structure of AgSi (111) Schottky diodes. *Surf. Sci.* **1995**, *324*, 249–256. [CrossRef]
59. Soylu, M.; Yakuphanoglu, F. Analysis of barrier height inhomogeneity in Au/n-GaAs Schottky barrier diodes by Tung model. *J. Alloy. Compd.* **2010**, *506*, 418–422. [CrossRef]